19 Lymphoproliferative Neoplasms

Clara G. C. Ooi and Ali Guermazi

CONTENTS

19.1 Introduction *337*
19.2 Leukemia *337*
19.3 Myeloid Sarcoma *339*
19.4 Hodgkin Disease *340*
19.5 Post-Transplantation Renal Allograft Lymphoproliferative Disorder *342*
19.6 AIDS-Related Lymphoma *344*
19.7 Waldenström Macroglobulinemia *344*
19.8 Multiple Myeloma and Plasmacytoma *344*
19.9 Conclusion *347*
References *347*

19.1 Introduction

The kidney is the fifth most commonly affected organ in myeloproliferative and lymphoproliferative disorders at autopsy (Barcos et al. 1987; Xiao et al. 1997). There is, however, a discrepancy between the incidence found at autopsy and that found clinically or on imaging (Eisenberg et al. 1994; Geoffay et al. 1984; Richmond et al. 1962; Rosenberg et al. 1961). This discrepancy has been explained by the supposition that renal involvement represents a late manifestation of the disease, and one which is frequently clinically asymptomatic unless infection or obstruction supervenes (Eisenberg et al. 1994). However, with improved technology in cross-sectional imaging, such as computed tomography (CT) and magnetic resonance (MR) imaging, and their increased utilization in the routine staging of hematological malignancies, the detection rate of renal involvement by these conditions will invariably rise (Eisenberg et al. 1994; Rosenberg et al. 1961; Reznek et al. 1990).

The prevalence of renal involvement at autopsy varies with the different hematological malignancies in question. It is reported in up to 45% of acute myeloid leukemia (AML), 38% of chronic myeloid leukemia (AML), 53% of acute lymphoblastic leukemia (ALL), and 60–90% of chronic lymphoblastic leukemia (CLL; Barcos et al. 1987; Schwartz and Shamsuddin 1981; Xiao et al. 1997). The incidence of lymphomatous infiltration of the kidney ranges from 33.5 to 62% at autopsy (Kiely et al. 1969; Martinez-Maldonado and Ramirez de Arellano 1966; Richmond et al. 1962; Xiao et al. 1997). Using radiographic techniques prior to the advent of CT (Ferry et al. 1995; Rosenberg et al. 1961), the incidence was reported to be less than 1%, but with CT it has increased to 8% (Chepuri et al. 2003; Cohan et al. 1990; Ellert and Kreel 1980; Geoffay et al. 1984; Hurii et al. 1983).

Extramedullary plasmacytoma of the kidney occurs either as a primary event without bone marrow involvement or as a manifestation of disseminated multiple myeloma and is extremely rare (Soesan et al. 1992). In an autopsy series of 120 cases of lymphoproliferative and myeloproliferative disorders, myelomatous involvement of the kidney was found in only 12% (Xiao et al. 1997).

Although renal involvement, such as urinary obstruction, uric acid, light-chain and drug-related nephropathies, glomerulopathies secondary to amyloidosis, cryoglobulinemia, and glomerulonephritis, is a common association in hematological malignancies, particularly the leukemias and myeloma, this chapter deals only with imaging of direct tumor infiltration or involvement of the kidney.

C. G. C. Ooi, MD
Associate Professor and Honorary Consultant, Department of Diagnostic Radiology, Queen Mary Hospital, University of Hong Kong, Room 405, Block K, Pokfulam Road, Hong Kong SAR, China
A. Guermazi, MD
Senior Radiologist, Scientific Director, Oncology Services, Department of Radiology Services, Synarc Inc., 575 Market Street, 17th Floor, San Francisco, CA 94105, USA

19.2 Leukemia

Although the kidney is one of the most common sites of involvement at autopsies in the leukemias, particularly lymphoblastic leukemia, radiological

evidence in the living patient is rarely encountered. The reason is most likely that up to 67% of renal involvement in leukemia is microscopic (Basker et al. 2002; Tanaka et al. 2004). When it occurs, renal involvement is more common at relapse than at initial presentation, as the kidneys, like the central nervous system and testes, are "sanctuary sites" where relapse may occur even in bone marrow remission (Tanaka et al. 2004). However, despite its prevalence in CLL, leukemic infiltration is rarely associated with renal failure and may therefore be clinically asymptomatic.

Interstitial infiltration by leukemic cells crowds out normal structures, and although both the renal medulla and cortex are usually involved simultaneously, Xiao et al. (1997) reported a predilection for the renal cortex in CLL with bilateral involvement more common than unilateral (Fig. 19.1).

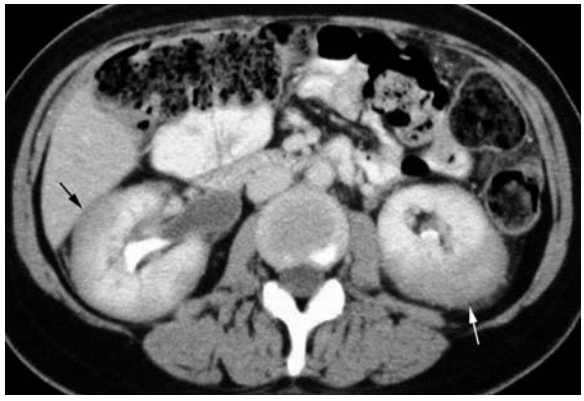

Fig. 19.1. Chronic lymphoblastic leukemia in a 51-year-old woman. Axial contrast-enhanced CT scan shows ill-defined hypodense lesions on both kidneys (*arrows*). (Image courtesy of P. Pickhardt)

There are four patterns of infiltration: bilateral diffuse renal infiltration; unilateral renal infiltration; focal masses; and perirenal/renal hilar infiltration.

Bilateral and diffuse renal enlargement with preservation of the reniform shape is the most common presentation (Boudville et al. 2001; Comerma-Coma et al. 1998; Gupta and Keane 1985; Parker 1997), although a lobulated appearance may be encountered (Basker et al. 2002). The bilateral diffuse renal enlargement can be observed on intravenous urography (IVU) with marked stretching of the calyces and infundibula (Gupta and Keane 1985) simulating polycystic kidneys; however, absence of cysts on cross-sectional imaging should exclude polycystic kidneys. On ultrasound (US), the infiltrated kidneys may be normal (Boudville et al. 2001; Parker 1997) or hypoechogenic (Gates 1978; Teele 1977), although cases of hyperechogenicity have been reported (Fig. 19.2) (Parker 1997). On CT, the bilateral diffuse infiltration is depicted as thickened renal parenchyma, which may be isodense or hypodense with compression of the pelvicalyceal system (Fig. 19.3; Araki 1982). The masses are minimally enhancing and remain hypodense relative to normal renal tissue after contrast administration (Fig. 19.4). These imaging features, however, are not specific and are also found with glycogen storage diseases and amyloidosis.

Unilateral diffuse renal enlargement can be confused with compensatory renal hypertrophy when renal function is unimpaired and with renal vein thrombosis when renal dysfunction is present (Araki 1982). In cases where there is bilateral but asymmetrical involvement, the smaller kidney may be erroneously diagnosed as normal on imaging.

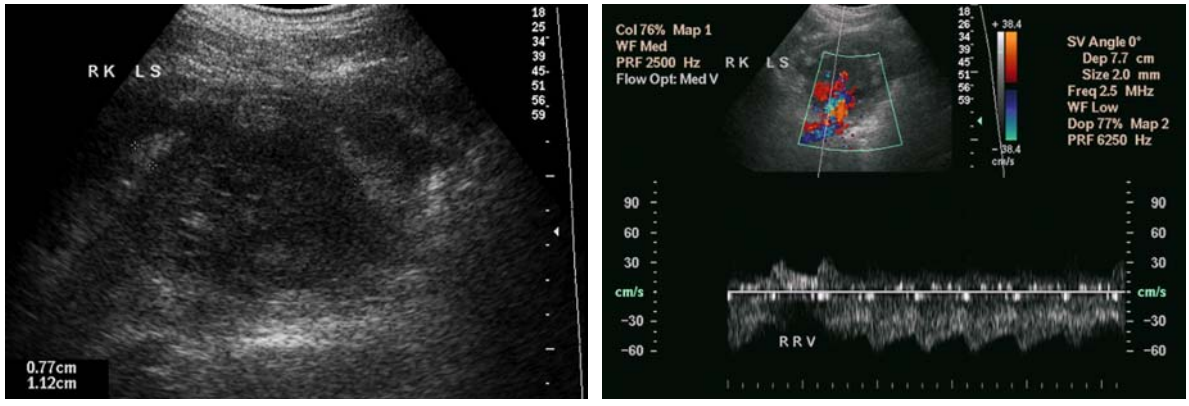

a b

Fig. 19.2a,b. Acute myeloblastic leukemia in a 59-year-old man. **a** Longitudinal ultrasound image of the right kidney shows echogenic tissue (*calipers*) surrounding the kidney in the perinephric space. **b** On Doppler ultrasound image, the renal hilar vessels are noted to be patent.

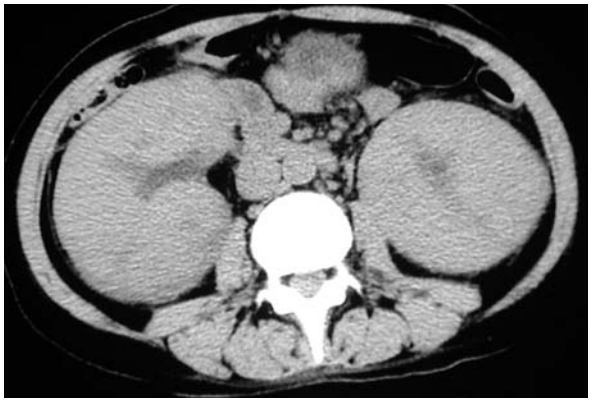

Fig. 19.3. Acute lymphoblastic leukemia in a 48-year-old woman who relapsed after bone marrow transplantation. Axial unenhanced CT scan of the abdomen shows bilateral diffuse renal enlargement by tissue isodense to muscle attenuation. Note para-aortic lymphadenopathy.

A third pattern of leukemic infiltration is the focal mass, which can be multiple, unilateral, or bilateral (Comerma-Coma et al. 1998; Teele 1977). The masses may appear hypoechoic on US (Goh et al. 1978) and hypodense on CT (Comerma-Coma et al. 1998; Teele 1977). This form of infiltration is rare in leukemia, although it is more common in lymphoma. The fourth pattern of leukemic renal infiltration manifests as enlarged peri-hilar or perirenal masses (Fig. 19.5), which may cause hydronephrosis and renal distortion (Teele 1977). These masses share the same US and CT characteristics as the other forms of renal leukemic infiltration.

19.3 Myeloid Sarcoma

Myeloid sarcoma, previously known as chloroma or granulocytic sarcoma, is an extremely rare extramedullary manifestation of myeloid leukemia (Vardiman et al. 2002). Myeloid sarcoma is defined as an extramedullary localized tumor composed of immature granulocytic precursors. Although usually associated with systemic disease in acute myeloid leukemia, granulocytic sarcoma may herald leukemic transformation in myelodysplastic disorders or diseases including chronic myeloid leukemia, polycythemia rubra vera, myelofibrosis, and chronic eosinophilic leukemia (Liu et al. 1973; Neiman et al. 1981). The overall incidence of myeloid sarcoma is 2.5–8%, and it is more common in children than in adults (13 vs 5%) with acute myeloid leukemia (Liu et al. 1973; Pui et al. 1994). There is a predilection for bone and perineural tissue (Neiman et al. 1981). Renal involvement is extremely rare and is usually reported at autopsy rather than in living patients (Breatnach 1985; Liu et al. 1973; Park et al. 2003). Renal myeloid sarcoma may manifest as diffuse enlargement of the affected kidney, which may be isodense or hypodense on CT, long-segment ureteral involvement, and enlarged retroperitoneal lymph node (Bagg et al. 1994; Breatnach 1985; Park et al. 2003).

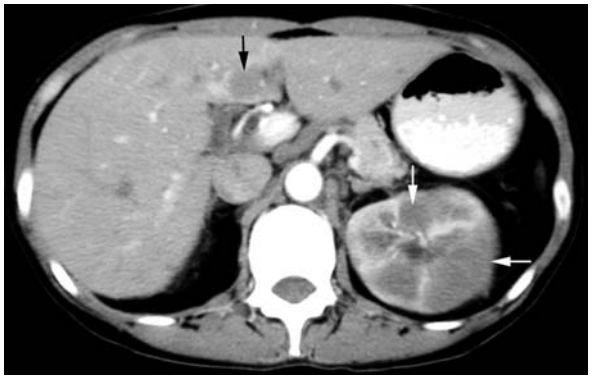

a

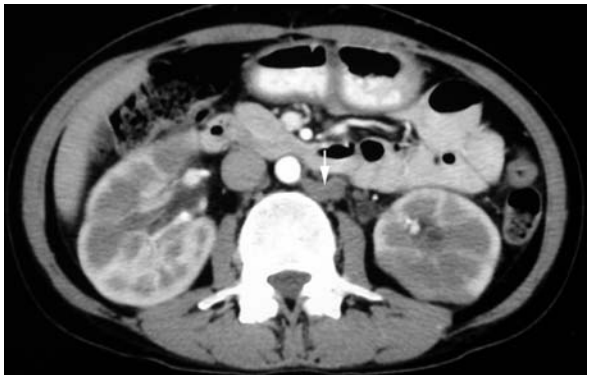

b

Fig. 19.4a,b. Acute lymphoblastic leukemia in a 52-year-old man. **a** Axial contrast-enhanced CT scan through the abdomen shows diffuse hypodense leukemic infiltration (*white arrows*) of the left kidney and a hypodense nodule (*black arrow*) in the segment IV of the liver. **b** Axial contrast-enhanced CT scan obtained caudad to **a** shows bilateral diffuse renal involvement and retroperitoneal lymphadenopathy (*arrow*).

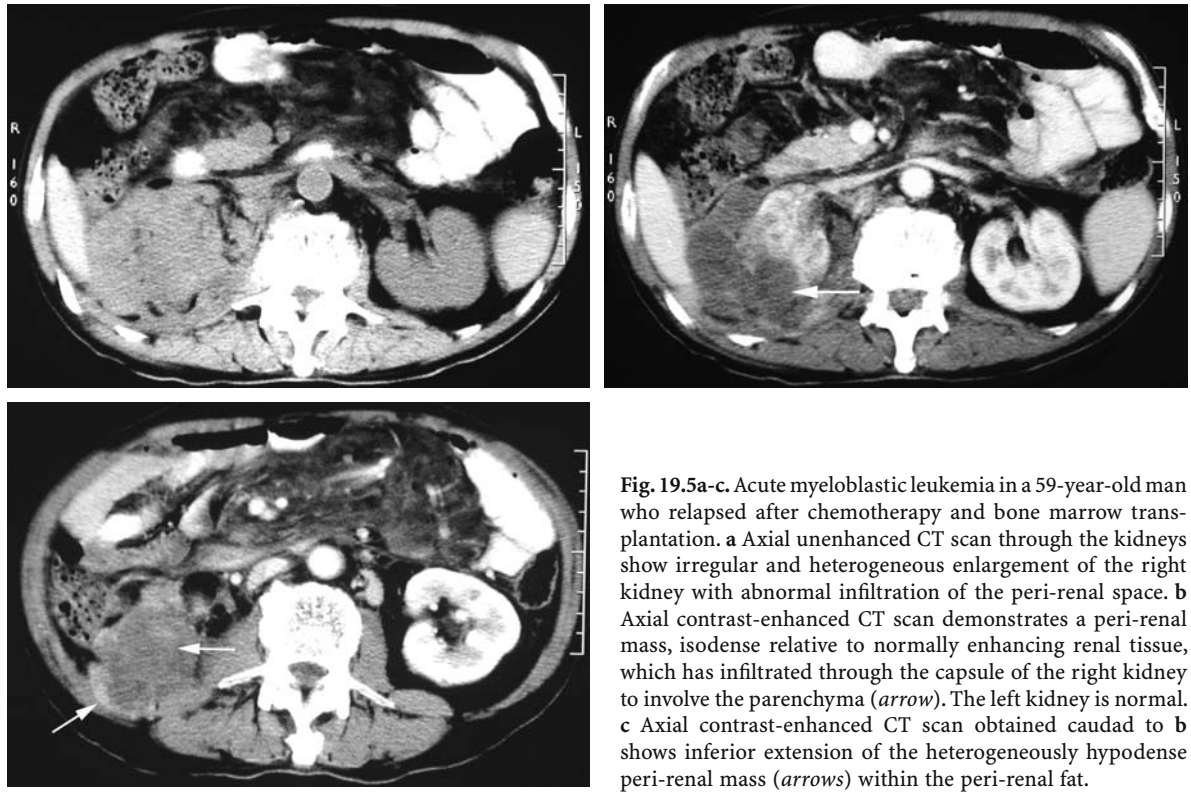

Fig. 19.5a-c. Acute myeloblastic leukemia in a 59-year-old man who relapsed after chemotherapy and bone marrow transplantation. **a** Axial unenhanced CT scan through the kidneys show irregular and heterogeneous enlargement of the right kidney with abnormal infiltration of the peri-renal space. **b** Axial contrast-enhanced CT scan demonstrates a peri-renal mass, isodense relative to normally enhancing renal tissue, which has infiltrated through the capsule of the right kidney to involve the parenchyma (*arrow*). The left kidney is normal. **c** Axial contrast-enhanced CT scan obtained caudad to **b** shows inferior extension of the heterogeneously hypodense peri-renal mass (*arrows*) within the peri-renal fat.

19.4 Hodgkin Disease

Renal involvement by non-Hodgkin lymphoma is common in disseminated disease, with an incidence of up to 62% at autopsy (Kiely et al. 1969; Martinez-Maldonado and Ramirez de Arellano 1966; Richmond et al. 1962; Xiao et al. 1997). It is, however, extremely rare and seldom encountered clinically in Hodgkin disease, being documented in less than 1% of patients at diagnosis (Cohan et al. 1990; Ferry et al. 1995; Pilatrino et al. 2003; Reznek et al. 1990). In general, lymphomatous infiltration is nearly always secondary to hematogenous spread or contiguous involvement from retroperitoneal lymphoma. Renal lymphoma arising de novo in the renal parenchyma as a primary tumor, and not from invasion of adjacent retroperitoneal lymphoma or as extranodal manifestation of disseminated lymphoma, is extremely rare. Due to the lack of specific symptoms, renal involvement in lymphoma is rarely diagnosed pre-operatively (Kandel et al. 1987) and is often diagnosed late in the disease. Symptoms cover the whole gamut of renal disease, but the most common are flank pain, hematuria, anemia, and weight loss. Imaging features are similar in Hodgkin and non-Hodgkin lymphoma of the kidneys.

The imaging features of renal lymphoma depend on the mechanism of spread to the kidney (hematogenous vs direct invasion), pattern of intrarenal growth (interstitial or expansile), and degree of extension beyond the kidney. Hematogenous seeding results in multiple nodular lesions in the renal parenchyma, which are localized to the cortex initially. Retroperitoneal lymphomatous masses involve the kidneys in two ways: via perinephric tissue with transcapsular spread through the renal capsule into the renal cortex or via the renal pelvis into the renal medulla (trans-sinus growth; Hartman et al. 1982). Once in the renal parenchyma, tumor infiltration is interstitial, growing in between the nephrons, blood vessels, and collecting ducts, using them as scaffolding. The kidneys maintain their reniform configuration and renal function during this phase, and on imaging, particularly on IVU, no or very subtle abnormalities are found (Cohan et al. 1990). Expansile growth follows with destruction of the "scaffolding" resulting in enlarged kidneys with compressed and deformed calyces. Uneven growth results in a lobulated outline with masses extending outside the renal contour. More commonly even growth results in multiple nodules in both kidneys. With continued growth there the entire renal parenchyma would be replaced.

In general, IVU is not a sensitive modality for evaluating renal lymphoma (Eisenberg et al. 1994). Computed tomography is the preferred modality for evaluating the kidney, its adjacent retroperitoneal space, and the rest of the abdomen. Five patterns of renal lymphoma have been described on CT: multiple renal masses (Fig. 19.6); direct invasion from contiguous retroperitoneal lymphoma; solitary focal masses (Fig. 19.7); diffuse infiltration (Fig. 19.8); and perirenal/perihilar disease. Multiple renal masses ranging from 1 to 3 cm, which can affect one or both kidneys, is most commonly followed by direct invasion of the kidney from contiguous retroperitoneal lymphomatous masses (Cohan et al. 1990; Heiken et al. 1983; Pilatrino et al. 2003; Reznek 1990). In general, renal lymphoma lesions are usually hypo- or isodense before contrast, and remain hypodense relative to normal-enhancing renal parenchyma after contrast administration (Chepuri et al. 2003; Cohan et al. 1990; Hartman et al. 1982; Pilatrino et al. 2003; Reznek 1990). On US, the lesions are hypoechoic with well-defined borders. Trans-sinus growth obliterates normally echogenic renal sinus fat, whereas perirenal lymphoma is depicted as a hypoechoic "halo" around the kidney (Cruz et al. 1995). Perirenal lymphoma results from trans-capsular spread from within the kidney or from infiltration by retroperitoneal disease (Cruz et al. 1995).

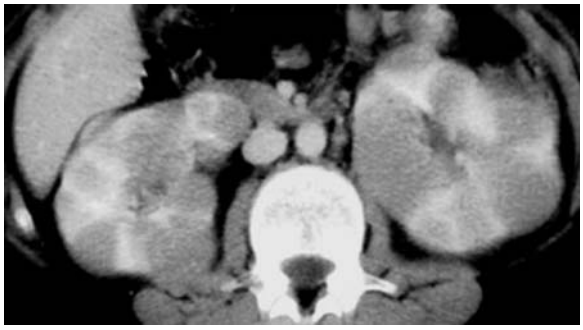

Fig. 19.6. Renal involvement by recurrent Hodgkin disease in a post-gestational 24-year-old woman. Axial contrast-enhanced CT scan shows bilateral involvement of the kidneys by several rounded hypodense lesions. This is a typical appearance of systemic involvement. Kidneys returned to normal after four chemotherapy courses of BEACOPP. (Image courtesy of L. Dobrovolskiene)

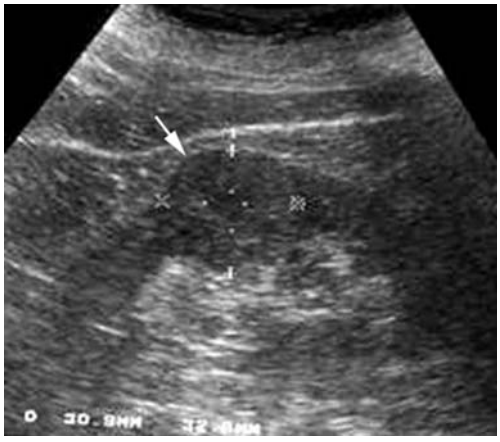

a

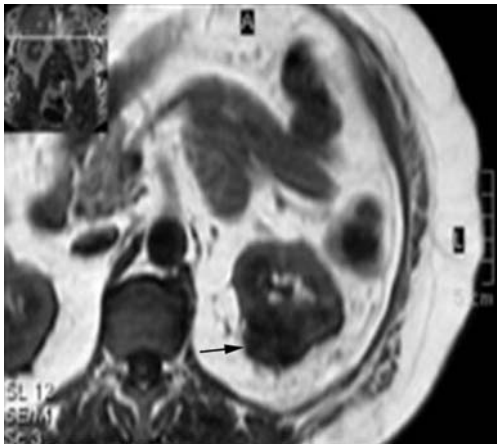

b

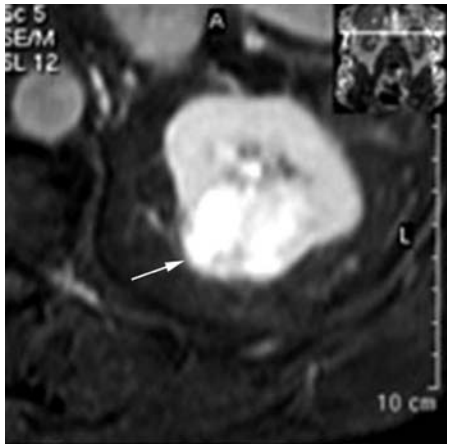

c

Fig. 19.7a-c. Stage IV Hodgkin disease of the kidney in a 62-year-old man with hematuria and enlarged mediastinal lymph nodes. **a** Longitudinal US image shows an isoechoic mass (*arrow*) of the left kidney deforming the renal contours. **b** Axial unenhanced T1-weighted MR image shows the mass (*arrow*) to be isointense to the renal parenchyma with **c** strong enhancement after contrast administration and fat suppression. Radiological imaging features were of renal cell carcinoma. Nephrectomy showed that the kidney was involved by Hodgkin disease.

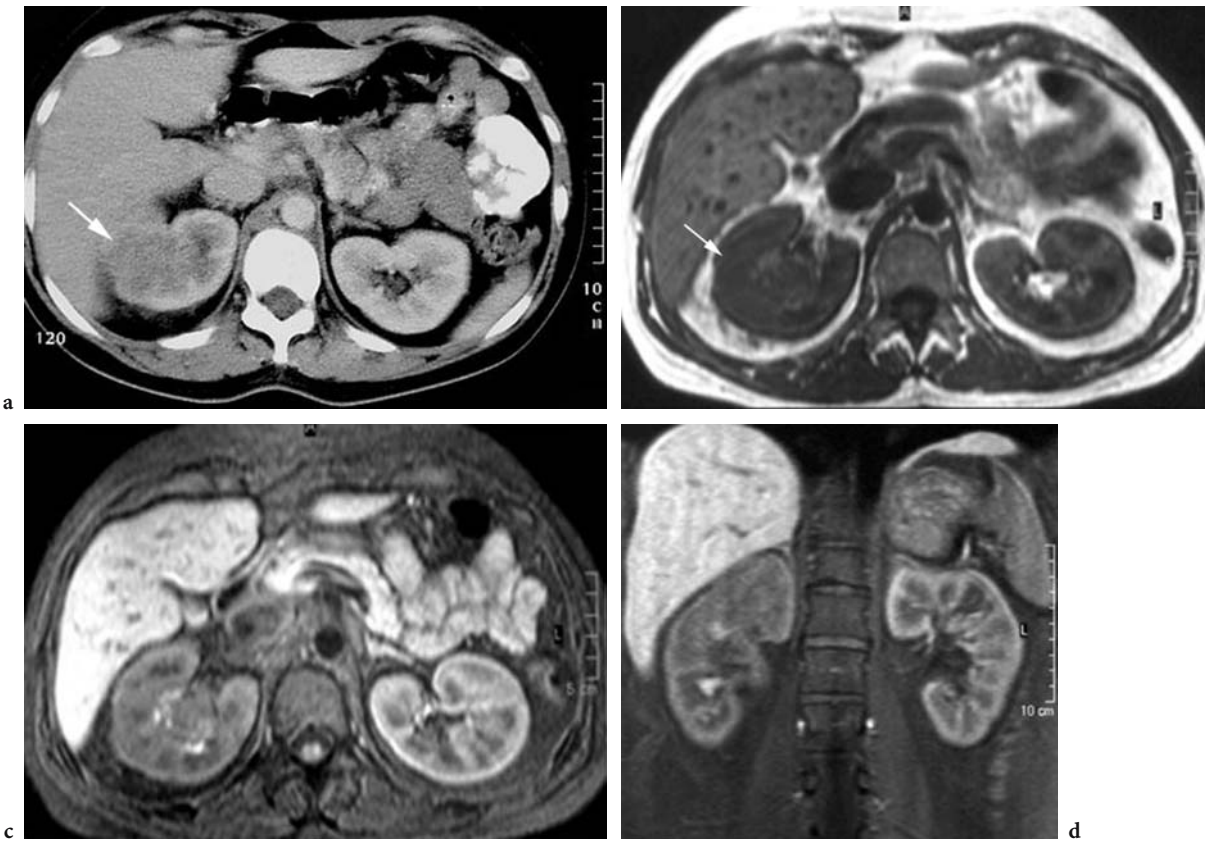

Fig. 19.8a-d. Infiltrative renal Hodgkin disease in a 32-year-old woman. **a** Axial contrast-enhanced CT scan shows hypodense infiltration (*arrow*) of the right kidney. The kidney is very slightly enlarged in comparison with the left kidney. **b** Axial unenhanced T1-weighted MR image shows the infiltration (*arrow*) to be slightly hypointense relative to the renal cortex. This infiltration obliterates the normally hyperintense renal sinus fat. **c** Axial and **d** coronal fat-suppressed contrast-enhanced T1-weighted MR images show minimal enhancement of the cortex of the right kidney due to diffuse infiltration. The reniform shape of the right kidney is maintained. (Image courtesy of L. Dobrovolskiene)

Gallium-67 citrate scanning has been used in the detection of lymphoma, with variable sensitivities depending on the site of involvement and cell type. It has the highest sensitivity (over 70%) in Hodgkin disease and diffuse large-cell malignant lymphoma, but poor sensitivity (<50%) in other cell types such as diffuse malignant lymphoma (Eisenberg et al. 1994; Hartman et al. 1982). The combination of single photon emission computed tomography (SPECT) with gallium scanning has been shown to be useful in differentiating lymphoma from benign tissue. Positron emission tomography (PET) has a better resolution than gallium scanning with increased sensitivity and shorter procedural time (Mavromatis and Cheson 2002). Its lack of specificity does not lend itself as an initial diagnostic tool in lymphoma, but it is useful in monitoring response (Romer and Schwaiger 1998).

19.5 Post-Transplantation Renal Allograft Lymphoproliferative Disorder

Post-transplantation lymphoproliferative disorders (PTLD) are a direct consequence of chronic immunosuppression, and their pathogenesis is strongly related to the Epstein-Barr virus (EBV). Most post-transplant malignancies are non-melanotic squamous cell carcinoma of the skin and lips (37%) followed by lymphomas (16%; Penn 1996). The incidence of PTLD varies with the organ transplanted. Due to aggressive immunosuppression, heart–lung transplantation has the highest incidence (4.6–25%) followed by liver (2.2–6.7%) and heart transplantations (1.8–5.1%; Penn 1996). The overall incidence of PTLD in renal transplants is 1–2%, which represents 21% of all malignancies in graft recipients

(Cockfield et al. 1993; Dodd et al. 1992; Lutz and Heemann 2003). The renal allograft is the most common site of PTLD (47%) after renal transplantation (Miller et al. 1997; Vose et al. 1996), although secondary involvement of the kidney from an extrarenal primary is also frequent (Frick et al. 1984). Non-Hodgkin lymphoma is the most common type of lymphoma to arise in renal allografts.

Although the imaging features of transplant lymphoma have been described as resembling those in non-transplant patients (Frick et al. 1984), a certain predilection for the allograft pedicle (Fig. 19.9) alludes to a predisposition for PTLD to occur at the anastomotic site (Ali et al. 1999; Lopez-Ben et al. 2000). Allograft pedicle involvement was described in 4 of 5 (80%), and 12 of 16, (75%) patients with renal allograft lymphoproliferative disorders (Ali et al. 1999; Lopez-Ben et al. 2000). Vascular encasement is a common feature. The PTLD masses are generally hypoechoic, although they may be heterogeneous at the renal hilum. On CT, they are hypodense masses (Fig. 19.9a) which can be non-enhancing, mildly enhancing, or peripherally enhancing (Lopez-Ben et al. 2000; Vrachliotis et al. 2000). Tumoral extension around the ureter from the renal pedicle can also be present (Fig. 19.9d). The MR findings include iso- to hypointensity on T1-weighted images and hypointensity on T2-weighted images, with mild and/or peripheral enhancement (Ali et al. 1999; Lopez-Ben et al. 2000). In the context of post-transplantation evaluation of a renal allograft, US is usually the initial modality. Presence of a complex mass, particularly at the hila, requires exclusion of non-neoplastic conditions such as resolving hematoma, seroma, abscesses, and complicated lymphocele, using other imaging techniques (Lopez-Ben et al. 2000). Doppler US is useful in delineating the relationship between renal hilar vessels and the mass. Both MR imaging and CT can further characterize renal masses and evaluate tumor extension, retroperitoneal lymphadenopathy, and involvement of other extranodal sites.

Differential diagnosis of masses located within and around the graft pedicle includes other compli-

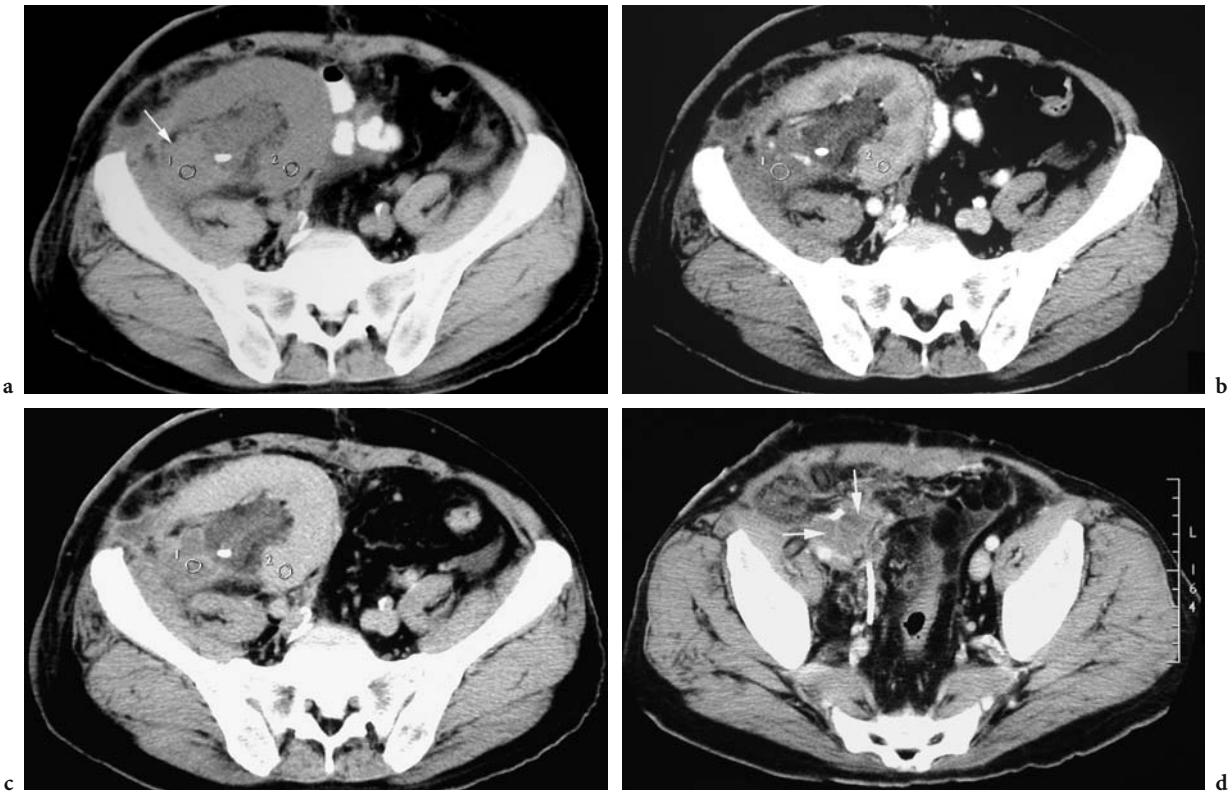

Fig. 19.9a-d. Post-transplantation lymphoproliferative disorder arising from the renal allograft in a 49-year-old woman. **a** Axial unenhanced CT scan through the pelvis shows a soft tissue thickening (*arrow*) at the renal pedicle. Note a JJ drainage stent at the pelviureteric junction. **b** Axial CT scan at the arterial phase of contrast administration show minimal contrast enhancement of the renal pedicle mass, which is hypodense relative to normally enhancing renal tissue and remains hypodense on **c** the venous phase of contrast administration. **d** The mass has extended inferiorly along and surrounding the ureter (*arrows*).

cations that occur after renal transplantation such as hematomas, perirenal lymphoceles, or abscesses (Claudon et al. 1998). Urinomas should be considered particularly in the presence of hydronephrosis.

19.6 AIDS-Related Lymphoma

Renal manifestations of acquired immunodeficiency syndrome (AIDS) include intrarenal infections, neoplastic disorders, acute tubular necrosis, glomerulonephritis, interstitial nephritis, and drug toxicity, among others (Miller et al. 1993). Compared with lymphoma in immunocompetent patients, AIDS-related lymphoma is much more aggressive and is associated with higher histological grades, wider extent of disease, greater incidence of extranodal disease, and poorer prognosis (Jeffrey et al. 1986; Siskin et al. 1995; Townsend et al. 1989). The liver and spleen are the two most common intraabdominal extranodal sites (up to 90%) of AIDS-related lymphoma on imaging, whereas renal involvement is reported in up to 12% of adults who are imaged (Clifton and Baily 1991; Moore et al. 1995; Nyberg et al. 1986; Siskin et al. 1995). AIDS-related lymphoma manifests as solitary or multiple discrete nodules that are hypoechoic on US and hypodense on CT (Nyberg et al. 1986; Siskin et al. 1995).

19.7 Waldenström Macroglobulinemia

Waldenström macroglobulinemia is a low-grade lymphoma characterized by malignant proliferation of mature plasmacytoid lymphocytes, which produce its hallmark monoclonal immunoglobulin M (IgM). The clinical presentation is a direct reflection of the effects of malignant infiltration of tissues, circulating IgM and tissue deposition of IgM. The bone marrow is the most common site of involvement followed by the reticuloendothelial system. Renal involvement is unusual and is reported in 6% of patients with this condition (Moore et al. 1995). Primary involvement is even rare (2.7%). Small nodular lesions and perinephric masses with imaging characteristics similar to other lymphomas have been reported (Fig. 19.10; Clifton and Baily 1991; Moore et al. 1995).

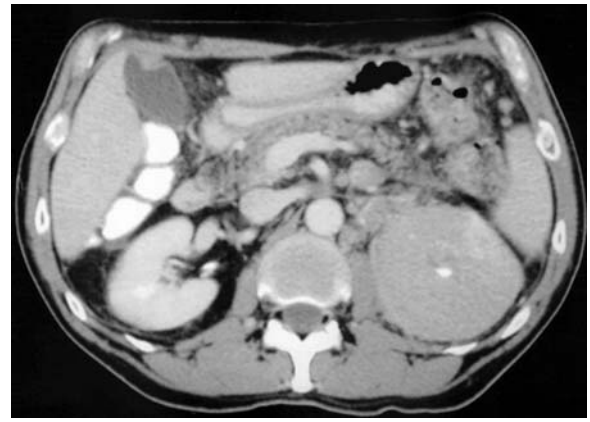

Fig. 19.10. Waldenström macroglobulinemia in a 70-year-old man with renal involvement. Axial contrast-enhanced CT scan of the abdomen shows hypodense left renal mass, which conforms to the contour of the kidney.

19.8 Multiple Myeloma and Plasmacytoma

Plasmacytoma is a malignant monoclonal proliferation of the B-cell line and a form of plasma cell tumor that can occur in any organ outside the bone marrow (Alexiou et al. 1999). Plasmacytoma may arise either from osseous (medullary) or non-osseous (extramedullary) sites (Alexiou et al. 1999; Bolek et al. 1996; Galieni et al. 1995; The International Myeloma Working Group 2003). Primary extramedullary plasmacytoma (EMP) is rare, accounting for 4% of all plasma cell tumors, and is defined as monoclonal plasma cell proliferation that develops in the absence of multiple myeloma elsewhere. Secondary EMP arises as an extramedullary manifestation of disseminated multiple myeloma. The EMP lesions classically arise in the upper aero-digestive tract (80%) with a predilection for the head and neck, followed by skin and gastrointestinal tract (Bolek et al. 1996; Igel et al. 1991; The International Myeloma Working Group 2003). Renal plasmacytoma is extremely rare (Alexiou et al. 1999).

Renal EMPs are vascular renal masses (Fig. 19.11; Igel et al. 1991; Kandel et al. 1984). In eight cases of renal plasmacytoma reviewed by Kandel et al. (1984), neovascularity was demonstrated in all five cases in which angiography was performed. Clinical presentations were also similar to those of renal cell carcinoma, the most common being palpable abdominal mass (50%) followed by gross hematuria (25%). Renal plasmacytomas can be large, associated with enlarged retroperitoneal lymph nodes (Fig. 19.12;

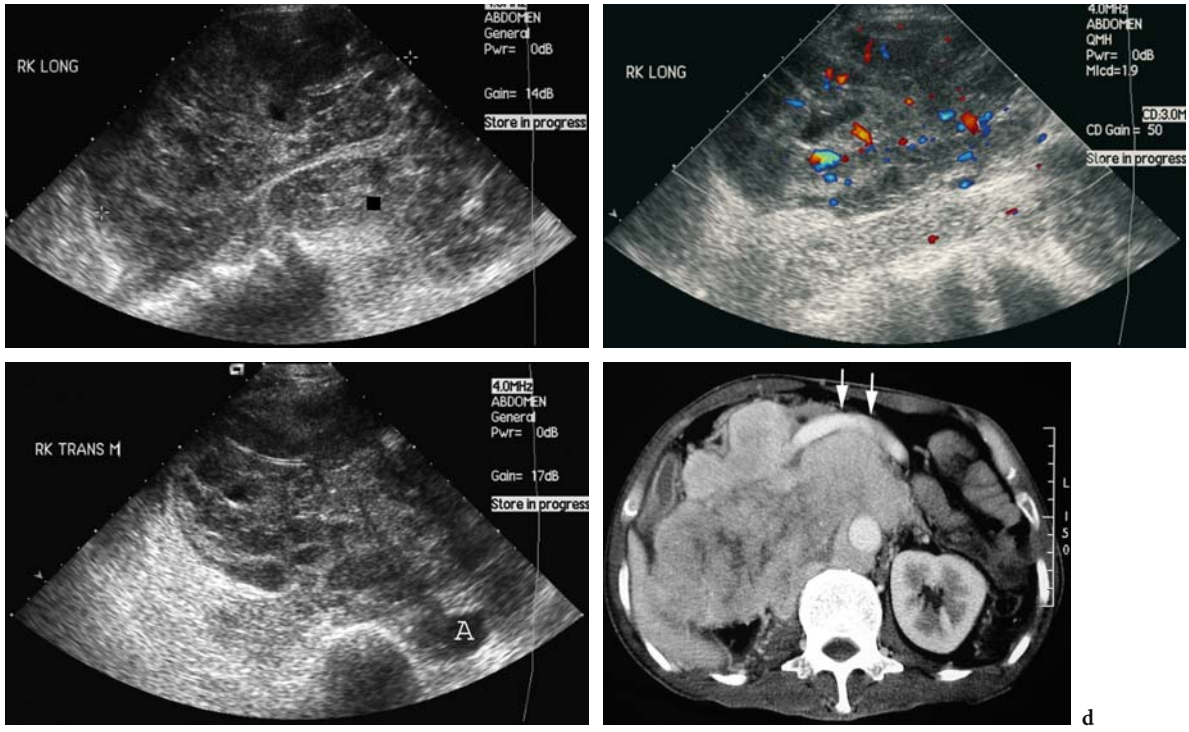

Fig. 19.11a-d. Extramedullary plasmacytoma arising from the right kidney in a 55-year-old woman. **a** Longitudinal US image of the right kidney shows diffuse replacement of normal renal tissue by a heterogeneous mass. **b** Color Doppler US image confirms vascularity of the mass. **c** Transverse US image of the right kidney illustrates the extent of the mass, which has displaced the aorta (*A*) to the left. **d** On axial contrast-enhanced CT scan, the mass is heterogeneously enhancing, and vascular encasement of the aorta and displacement of the portal vein (*arrows*) are better represented.

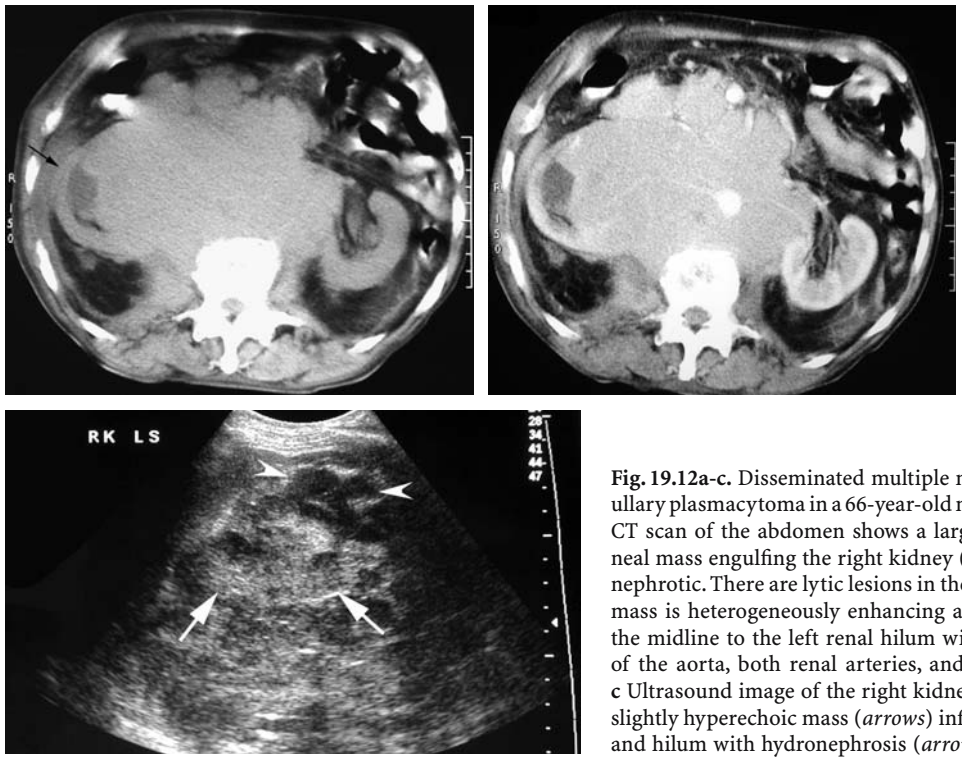

Fig. 19.12a-c. Disseminated multiple myeloma and extramedullary plasmacytoma in a 66-year-old man. **a** Axial unenhanced CT scan of the abdomen shows a large isodense retroperitoneal mass engulfing the right kidney (*arrow*), which is hydronephrotic. There are lytic lesions in the lumbar vertebra. **b** The mass is heterogeneously enhancing and has extended across the midline to the left renal hilum with vascular encasement of the aorta, both renal arteries, and root of the mesentery. **c** Ultrasound image of the right kidney shows heterogeneous, slightly hyperechoic mass (*arrows*) infiltrating the renal pelvis and hilum with hydronephrosis (*arrowheads*).

Kanoh et al. 1993), vascular encasement (Figs. 19.11, 19.12), and involvement of the renal vein (Jaspan and Gregson 1984; Sered and Nikolaidis 2003). Other manifestations include masses arising from the perinephric area (Figs. 19.13, 19.14; Sered and Nikolaidis 2003) similar to lymphoma or metastases, and the renal pelvis simulating transitional cell carcinoma (Igel et al. 1991; Kandel et al. 1984). Renal plasmacytomas have heterogeneous echogenicity on US (Figs. 19.11, 19.12), are isodense on unenhanced CT, and demonstrate heterogeneous enhancement, which can simulate renal cell carcinoma (Figs. 19.11, 19.15, 19.16). Ultrasound, CT, IVU, and angiography have thus far been unable to differentiate renal plasmacytomas from other malignant renal masses, particularly renal or transitional cell carcinoma (Igel et al. 1991; Kandel et al. 1984; Solomito and Grise 1972); however, in the presence of Bence-Jones proteinuria,

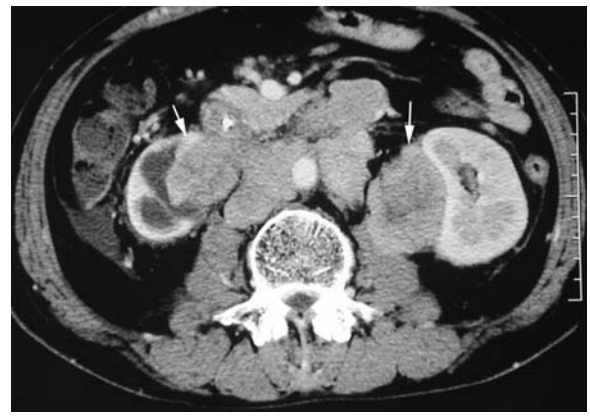

Fig. 19.13. Multiple myeloma complicated by extramedullary plasmacytoma in a 46-year-old man. Axial contrast-enhanced CT scan shows enhancing perinephric masses (*arrows*) at the medial aspects of the kidneys, with retroperitoneal lymphadenopathy. There is hydronephrosis of the right kidney.

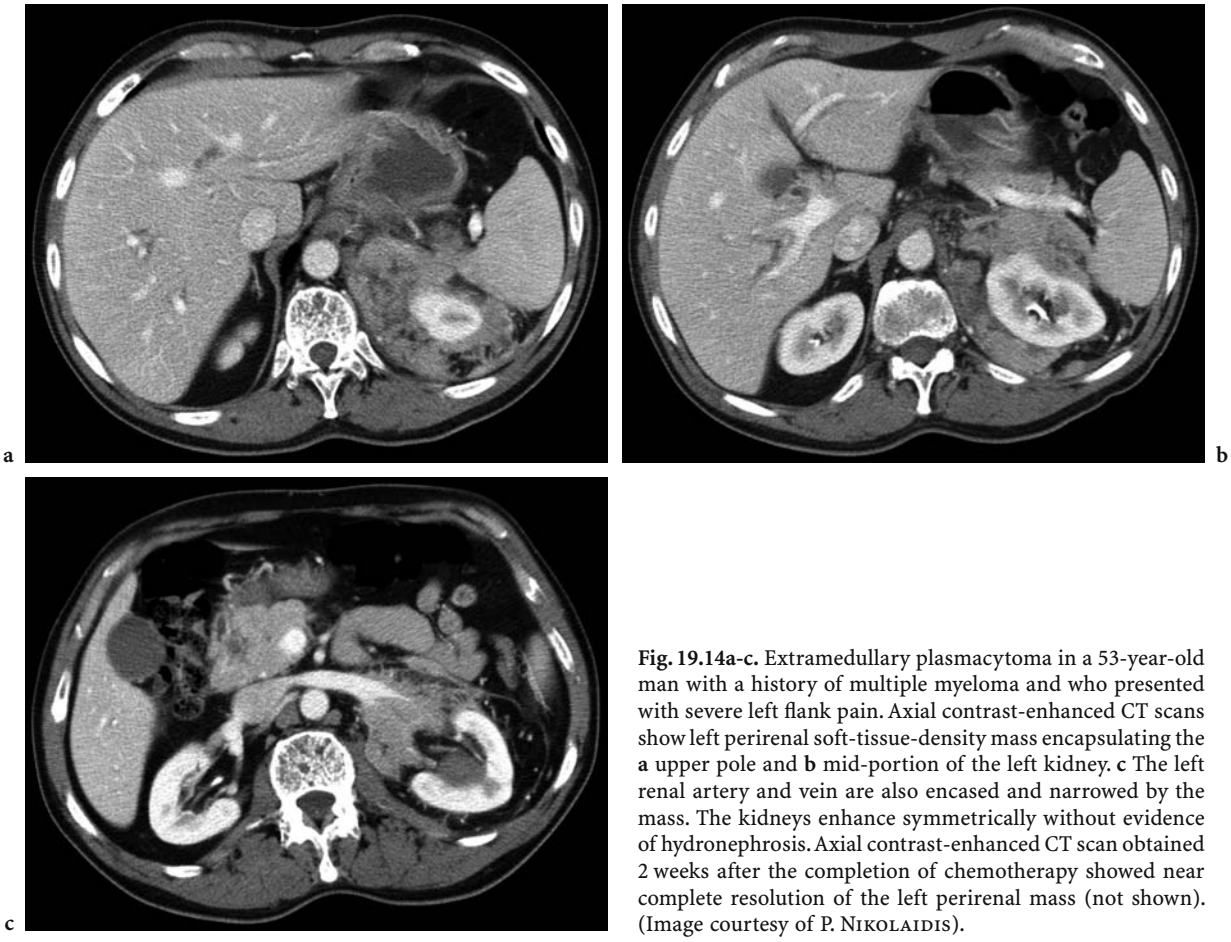

Fig. 19.14a-c. Extramedullary plasmacytoma in a 53-year-old man with a history of multiple myeloma and who presented with severe left flank pain. Axial contrast-enhanced CT scans show left perirenal soft-tissue-density mass encapsulating the **a** upper pole and **b** mid-portion of the left kidney. **c** The left renal artery and vein are also encased and narrowed by the mass. The kidneys enhance symmetrically without evidence of hydronephrosis. Axial contrast-enhanced CT scan obtained 2 weeks after the completion of chemotherapy showed near complete resolution of the left perirenal mass (not shown). (Image courtesy of P. Nikolaidis).

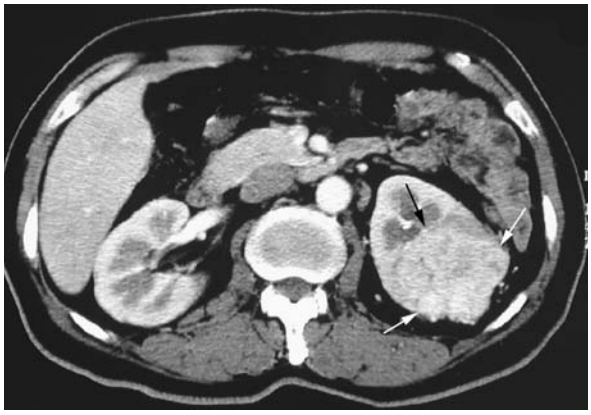

Fig. 19.15. Renal plasmacytoma in a 58-year-old man without bone marrow evidence of multiple myeloma. Axial contrast-enhanced CT scan shows a heterogeneously enhancing mass (*arrows*) arising from the left kidney.

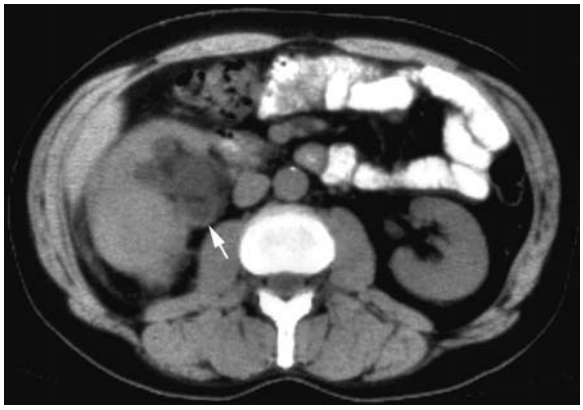

a

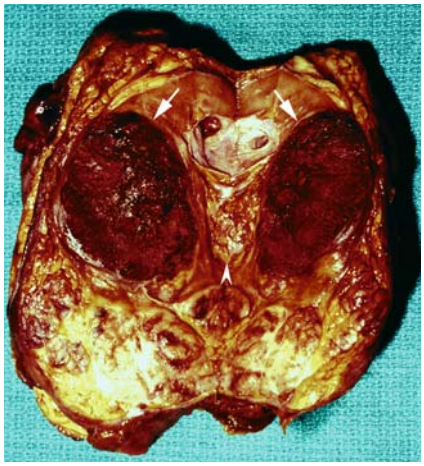

b

Fig. 19.16a,b. Renal plasmacytoma in a 59-year-old man with a recent significant weight loss. **a** Axial unenhanced CT scan shows an enlarged and irregular right kidney with a hypodense and lobulated mass (*arrow*) in the region of the renal hilum. **b** Photograph of the bivalved specimen shows the mass (*arrows*) in the mid-portion of the kidney, with extension into the renal pelvis (*arrowhead*). (Image courtesy of G. Lonergan)

and/or history of previous plasmacytoma or multiple myeloma, the presence of a documented renal mass should raise the suspicion of a renal plasmacytoma.

19.9 Conclusion

Renal involvement in myeloproliferative and lymphoproliferative disorders is generally not routinely imaged, as in most instances they are asymptomatic owing to preserved renal function. Symptoms arise as a result of compression, renal obstruction, infection, or hemorrhage. Ultrasound and CT remain the imaging modalities of choice due to their availability, relatively short scan times, and reduced costs compared with MR imaging. Computed tomography in particular is extremely good at depicting renal, perirenal, and intra-abdominal pathology. However, nuclear medicine imaging, particularly PET, is proving useful in post-treatment monitoring of disease activity. Although there are no specific imaging features that differentiate these entities from other disease processes that can affect the kidney, in general, leukemia and lymphoma are iso- or hypoechoic on US, and iso- or hypodense on CT. Lymphomas are hypovascular, showing minimal or no enhancement after contrast administration on CT. Extramedullary plasmacytomas are heterogeneous on US, isodense on CT, and demonstrate heterogeneous enhancement.

Acknowledgements
We extend sincere thanks to L. Dobrovolskiene, G. Lonergan, P. Nikolaidis, and P. Pickhardt for providing us with their excellent images.

References

Alexiou C, Kau RJ, Dietzfelbinger H, Kremer M, Spiess JC, Schratzenstaller B, Arnold W (1999) Extramedullary plasmacytoma: tumor occurrence and therapeutic concepts. Cancer 85:2305–2314

Ali MG, Coakley FV, Hricak H, Bretan PN (1999) Complex posttransplantation abnormalities of renal allografts: evaluation with MR imaging. Radiology 211:95–100

Araki T (1982) Leukemic ivolvement of the kidney in children: CT features. J Comput Assist Tomogr 6:781–784

Bagg MD, Wettlaufer JN, Willadsen DS, Ho V, Lane D, Thrasher JB (1994) Granulocytic sarcoma presenting as a diffuse renal mass before hematological manifestations of acute myelogenous leukemia. J Urol 152:2092–2093

Barcos M, Lane W, Gomez GA, Han T, Freeman A, Preisler H, Henderson E (1987) An autopsy study of 1206 acute and chronic leukemias (1958 to 1982). Cancer 60:827–837

Basker M, Scott JX, Ross B, Kirubakaran C (2002) Renal enlargement as primary presentation of acute lymphoblastic leukaemia. Indian J Cancer 39:154–156

Bolek TW, Marcus RD, Mendenhall NP (1996) Solitary plasmacytoma of bone and soft tissue. Int J Radiat Oncol Biol Phys 36:329–333

Boudville N, Latham B, Cordingly F, Warr K (2001) Renal failure in a patient with leukaemic infiltration of the kidney and polyomavirus infection. Nephrol Dial Transplant 16:1059–1061

Breatnach E, Stanley RJ, Carpenter JT Jr (1985) Intrarenal chloroma causing obstructive nephropathy: CT characteristics. J Comput Assist Tomogr 9:822–824

Chepuri NB, Strouse PJ, Yanik GA (2003) CT of renal lymphoma in children. Am J Roentgenol 180:429–431

Claudon M, Kessler M, Champigneulle J, Lefevre F, Hestin D, Renoult E (1998) Lymphoproliferative disorders after renal transplantation: role of medical imaging. Eur Radiol 8:1686–1693

Clifton AG, Baily GG (1991) Case report: renal lymphoma in a patient with Waldenstrom's macroglobulinemia. Clin Radiol 43:285–286

Cockfield SM, Preiksaitis JK, Jewell LD, Parfrey NA (1993) Post-transplant lymphoproliferative disorder in renal allograft recipients. Clinical experience and risk factor analysis in a single center. Transplantation 56:88–96

Cohan RH, Dunnick NR, Leder RA, Baker ME (1990) Computed tomography of renal lymphoma. J Comput Assist Tomogr 14:933–938

Comerma-Coma MI, Sans-Boix A, Tuset-Andujar E, Andreu-Navarro J, Perez-Ruiz A, Naval-Marcos I (1998) Reversible renal failure due to specific infiltration of the kidney in chronic lymphatic leukaemia. Nephrol Dial Transplant 13:1550–1552

Cruz Villalon F, Escribano Fernandez J, Ramirez Garcia T (1995) The hypoechoic halo: a finding in renal lymphoma. J Clin Ultrasound 23:379–381

Dodd GD III, Greenler DP, Confer SR (1992) Thoracic and abdominal manifestations of lymphoma occurring in the immunocompromised patient. Radiol Clin North Am 30:597–610

Eisenberg PJ, Papanicolaou N, Lee MJ, Yoder IC (1994) Diagnostic imaging in the evaluation of renal lymphoma. Leuk Lymphoma 16:37–50

Ellert J, Kreel L (1980) The role of computed tomography in the initial staging and subsequent management of the lymphomas. J Comput Assist Tomogr 4:368–391

Ferry JA, Harris NL, Papanicolau N, Young RH (1995) Lymphoma of the kidney. A report of 11 cases. Am J Surg Pathol 19:134–144

Frick MP, Salomonowitz E, Hanto DW, Gedgaudas-McClees K (1984) CT of abdominal lymphoma after renal transplantation. Am J Roentgenol 142:97–99

Galieni P, Cavo M, Avvisati G, Pulsoni A, Falbo R, Bonelli MA, Russo D, Petrucci MT, Bucalossi A, Tura S (1995) Solitary plasmacytoma of bone and extramedullary plasmacytoma: Two different entities? Ann Oncol 6:687–691

Gates GF (1978) Atlas of abdominal ultrasonography in children. Churchill Livingston, New York

Geoffay A, Shirkhoda A, Wallace S (1984) Abdominal and pelvic computed tomography in leukemic patients. J Comput Assist Tomogr 8:857–860

Goh TS, LeQuesne GW, Wong KY (1978) Severe infiltration of the kidneys with ultrasonic abnormalities in acute lymphoblastic leukemia. Am J Dis Child 132:1024–1025

Gupta S, Keane S (1985) Renal enlargement as a primary presentation of acute lymphoblastic leukaemia. Br J Radiol 58:893–895

Hartman DS, Davis CJ Jr, Goldman SM, Friedman AC, Fritzsche P (1982) Renal lymphoma: radiologic–pathologic correlation of 21 cases. Radiology 144:759–766

Heiken JP, Gold RP, Schnur MJ, King DL, Bashist B, Glazer HS (1983) Computed tomography of renal lymphoma with ultrasound correlation. J Comput Assist Tomogr 7:425–450

Hurii SC, Bosniak MA, Megibow AJ, Raghavendra BN (1983) Correlation of CT and ultrasound in the evaluation of renal lymphoma. Urol Radiol 5:69–76

Igel TC, Engen DE, Banks PM, Keeney GL (1991) Renal plasmacytoma: Mayo Clinic experience and review of the literature. Urology 37:385–389

Jaspan T, Gregson R (1984) Extramedullary plasmacytoma of the kidney. Br J Radiol 57:95–97

Jeffrey RB Jr, Nyberg DA, Bottles K, Abrams DI, Federle MP, Wall SD, Wing VW, Laing FC (1986) Abdominal CT in acquired immunodeficiency syndrome. Am J Roentgenol 146:7–13

Kandel LB, Harrison LH, Woodruff RF, Williams CD, Ahl ET Jr (1984) Renal plasmacytoma: a case report and summary of reported cases. J Urol 132:1167–1169

Kandel LB, McCullough DL, Harrison LH, Woodruff RD, Ahl ET Jr, Munitz HA (1987) Primary renal lymphoma. Does it exist? Cancer 60:386–391

Kanoh T, Katoh H, Izumi T, Tsuji M, Okuma M (1993) Renal plasmacytoma. Rinsho Ketsueki 34:1470–1473

Kiely JM, Wagoner RD, Holley KE (1969) Renal complications of lymphoma. Ann Intern Med 71:1159–1175

Liu PI, Ishimaru T, McGregor DH, Okada H, Steer A (1973) Autopsy study of granulocytic sarcoma (chloroma) in patients with myelogenous leukemia, Hiroshima–Nagasaki 1949–1969. Cancer 31:948–955

Lopez-Ben R, Smith JK, Kew CE II, Kenney PJ, Julian BA, Robbin ML (2000) Focal posttransplantation lymphoproliferative disorder at the renal allograft hilum. Am J Roentgenol 175:1417–1422

Lutz J, Heemann U (2003) Tumours after kidney transplantation. Curr Opin Urol 13:105–109

Martinez-Maldonado M, Ramirez de Arellano GA (1966) Renal involvement in malignant lymphoma: a survey of 49 cases. J Urol 95:485–488

Mavromatis BH, Cheson BD (2002) Pre- and post-treatment evaluation of non-Hodgkin's lymphoma. Best Pract Res Clin Haematol 15:429–447

Miller FH, Parikh S, Gore RM, Nemcek AA Jr, Fitzgerald SW, Vogelzang RL (1993) Renal manifestations of AIDS. Radiographics 13:587–596

Miller WT Jr, Siegel SG, Montone KT (1997) Post transplantation lymphoproliferative disorder: changing manifestation of disease in a renal transplant population. Crit Rev Diagn Imaging 36:569–585

Moore DF, Moulopoulos LA, Dimopoulos MA (1995) Waldenstrom's macroglobulinemia presenting as a renal or perirenal mass: clinical and radiographic features. Leuk Lymphoma 17:331–334

Neiman RS, Barcos M, Berard C, Bonner H, Mann R, Rydell RE, Bennett JM (1981) Granulocytic sarcoma: a clinicopathologic study of 61 biopsied cases. Cancer 48:1426–1437

Nyberg DA, Jeffrey RB Jr, Federle MP, Bottles K, Abrams DI (1986) AIDS-related lymphomas: evaluation by abdominal CT. Radiology 159:59–63

Park HJ, Jeong DH, Song HG, Lee GK, Han GS, Cha SH, Ha TS (2003) Myeloid sarcoma of both kidneys, the brain and multiple bones in a non-leukemic child. Yonsei Med J 44:740–743

Parker BR (1997) Leukemia and lymphoma in childhood. Radiol Clin North Am 35:1495–1516

Penn I (1996) Cancers in cyclosporin-treated vs azathioprine-treated patients. Transplant Proc 28:876–878

Pilatrino C, Cataldi A, Guerrasio A, Saglio G (2003) Images in haematology. Renal Hodgkin's disease. Br J Haematol 116:732

Pui MH, Fletcher BD, Langston JW (1994) Granulocytic sarcoma in childhood leukemia: imaging features. Radiology 190:698–702

Reznek RH, Mootoosamy I, Webb JA, Richards MA (1990) CT in renal and perirenal lymphoma: a further look. Clin Radiol 42:233–238

Richmond J, Sherman RS, Diamond HD, Craver LF (1962) Renal lesions associated with malignant lymphomas. Am J Med 32:184–207

Romer W, Schwaiger M (1998) Positron emission tomography in diagnosis and therapy monitoring of patients with lymphoma. Clin Positron Imaging 1:101–110

Rosenberg SA, Diamond HD, Jaslowitz B, Craver LF (1961) Lymphosarcoma: a review of 1269 cases. Medicine (Baltimore) 40:31–84

Schwartz JB, Shamsuddin AM (1981) The effects of leukemic infiltrates in various organs in chronic lymphocytic leukemia. Hum Pathol 12:432–440

Sered S, Nikolaidis P (2003) CT findings of perirenal plasmacytoma. Am J Roentgenol 181:888

Siskin GP, Haller JO, Miller S, Sundaram R (1995) AIDS-related lymphoma: radiologic features in pediatric patients. Radiology 196:63–66

Soesan M, Paccagnella A, Chiarion-Sileni V, Salvagno L, Fornasiero A, Sotti G, Zorat PL, Favaretto A, Fiorentino M (1992) Extramedullary plasmacytoma: clinical behaviour and response to treatment. Ann Oncol 3:51–57

Solomito VL, Grise J (1972) Angiographic findings in renal (extramedullary) plasmacytoma: case report. Radiology 102:559–560

Tanaka N, Matsumoto T, Furukawa M, Tokuda O (2004) Leukemia. In: Guermazi A (ed) Radiological imaging in hematological malignancies. Springer, Berlin Heidelberg New York, pp 351–366

Teele RL (1977) Ultrasonography of the genitourinary tract in children. Radiol Clin North Am 15:109–128

The International Myeloma Working Group (2003) Criteria for the classification of monoclonal gammopathies, multiple myeloma and related disorders: a report of the International Myeloma Working Group. Br J Haematol 121:749–757

Townsend RR, Laing FC, Jeffrey RB Jr, Bottles K (1989) Abdominal lymphoma in AIDS: evaluation with US. Radiology 171:719–724

Vardiman JW, Harris NL, Brunning RD (2002) The World Health Organization (WHO) classification of the myeloid neoplasms. Blood 100:2292–2302

Vose JM, Bierman PJ, Anderson JR, Harrison KA, Dalrymple GV, Byar K, Kessinger A, Armitage JO (1996) Single-photon emission computed tomography gallium imaging versus computed tomography: predictive value in patients undergoing high-dose chemotherapy and autologous stem-cell transplantation for non-Hodgkin's lymphoma. J Clin Oncol 14:2473–2479

Vrachliotis TG, Vaswani KK, Davies EA, Elkhammas EA, Bennett WF, Bova JG (2000) CT findings in posttransplantation lymphoproliferative disorder of renal transplants. Am J Roentgenol 175:183–188

Xiao JC, Walz-Mattmuller R, Ruck P, Horny HP, Kaiserling E (1997) Renal involvement in myeloproliferative and lymphoproliferative disorders. A study of autopsy cases. Gen Diagn Pathol 142:147–153